Anomalous Absorption Line in the Magneto-Optical Response of Graphene

V.P. Gusynin[1], S.G. Sharapov[2], and J.P. Carbotte[2]

[1] *Bogolyubov Institute for Theoretical Physics, 14-b Metrologicheskaya Street, Kiev, 03143, Ukraine*
[2] *Department of Physics and Astronomy, McMaster University, Hamilton, Ontario, Canada, L8S 4M1*
(Dated: February 6, 2008)

The intensity as well as position in energy of the absorption lines in the infrared conductivity of graphene, both exhibit features that are directly related to the Dirac nature of its quasiparticles. We show that the evolution of the pattern of absorption lines as the chemical potential is varied encodes the information about the presence of the anomalous lowest Landau level. The first absorption line related to this level always appears with full intensity or is entirely missing, while all other lines disappear in two steps. We demonstrate that if a gap develops, the main absorption line splits into two provided that the chemical potential is greater than or equal to the gap.

While graphene has only recently been isolated[1], several anomalous dc properties already appear well established[2,3,4]. This includes an unconventional integer quantum Hall effect with filling factor $\nu = \pm 2, \pm 6, \pm 10, \dots$[2,3,5,6,7] which changes to $\nu = 0, \pm 1, \pm 2, \pm 4, \dots$ at a magnetic field B above 20 T Ref.[4], which may indicate an opening of a gap. Also observed is a Berry phase of π[2,3,6] which increases to 2π in bilayers[8]. These spectacular dc properties can be traced to the nature of the quasiparticles in graphene which are massless Dirac fermions governed by $2+1$ dimensional quantum electrodynamics[9,10]. Optical conductivity measurements play a central role in solid state physics and have provided additional information on the dynamics of charge carriers and its change under external perturbations, not directly available in dc measurements. Here we present a theory of the diagonal optical conductivity of Dirac quasiparticles in an external magnetic field and highlight several unusual features, not present in a conventional two dimensional electron gas, which bear directly on their unconventional dynamics. We also investigate an emerging new physics of graphene related to the sublattice symmetry breaking reported in Ref.[4].

In the presence of a magnetic field, Landau levels (LLs) form in the electronic density of states and transitions between these levels give rise to absorption lines in the optical conductivity. In this letter we find that the selection rules, which set the frequencies of the lines and their relative spectral weight, provide a distinct signature of the presence of the Dirac quasiparticles. Not only do the positions and the intensities of the absorption lines scale with $\sqrt{B}$ rather than B, but the line corresponding to the transition from the lowest, $n=0$ to the $n=1$ (Landau level) LL is anomalous due to the special Dirac character of the $n=0$ level. This level and no others can participate in both inter and intraband transitions. As a consequence, the first absorption line always appears with full intensity or is entirely missing, while all other lines can also be seen to have in addition half intensity depending on the position of chemical potential μ relative to the LL energies. The chemical potential μ is tunable in experiments by application of a gate bias voltage to a field effect device[1,2,3,4].

Expressions for the absorptive part of the diagonal as well as Hall conductivity on which our calculations are based can be found in[7,11,12]. In the limit of zero impurity scattering rate, $\Gamma \to 0$, the diagonal conductivity as a function of the photon energy Ω is

$$\mathrm{Re}\,\sigma_{xx}(\Omega) = \frac{e^2}{h}\frac{2v_F^2|eB|\hbar}{c\Omega}\frac{\pi}{2}\times$$
$$\sum_{n=0}^{\infty}\left[\left(1+\frac{\Delta^2}{M_n M_{n+1}}\right)A(T)\delta(M_n + M_{n+1} - \Omega)\right. \quad (1)$$
$$\left.+\left(1-\frac{\Delta^2}{M_n M_{n+1}}\right)B(T)\delta(M_n - M_{n+1} + \Omega)\right],$$

where the thermal factors are $A(T) = n_F(-M_{n+1}) - n_F(M_n) + n_F(-M_n) - n_F(M_{n+1})$ and $B(T) = n_F(M_n) - n_F(M_{n+1}) + n_F(-M_{n+1}) - n_F(-M_n)$ with the Fermi distribution $n_F(\omega) = [\exp[(\omega - \mu)/T] + 1]^{-1}$ (we set the Boltzmann constant $k_B = 1$). To include damping, the n'th delta function in Eq. (1) is replaced by a Lorentzian of width $\Gamma_n + \Gamma_{n+1}$ with Γ_n the width of n'th level. Also in Eq. (1) a term $\Omega \to -\Omega$ is to be subtracted. In the presence of an excitonic gap Δ[13,14] the LL energies are $E_n = \pm M_n$, with $M_n = \sqrt{\Delta^2 + 2n|eB|\hbar v_F^2/c}$, and v_F is the Fermi velocity in graphene, $\hbar$ is Planck's constant h over 2π, c is the velocity of light and e is the charge of the electron. The field B is applied perpendicular to the plane and for $B = 1\,\mathrm{T}$ the energy scale $M_1 \approx 420\,\mathrm{K}$ for $v_F \approx 10^6\,\mathrm{m/s}$ and $\Delta = 0$. As for the conventional case, the selection rules allow transitions only between adjacent LLs (see Ref.[11] for details).

Our numerical results for $\mathrm{Re}\,\sigma_{xx}(\Omega)$ are given in Fig. 1 (a), where it is plotted in units e^2/h as a function of Ω for $\Delta = 0$. The same constant electronic scattering rate $\Gamma = 15\mathrm{K}$[4] was used for all LLs, an assumption that could easily be relaxed. Except for the long dashed (red) curve for which the magnetic field $B = 10^{-4}\mathrm{T}$, and is shown only for comparison, $B = 1\mathrm{T}$ for other curves. They differ only in value of chemical potential μ. The dash-dotted (black) curve has $M_0 < \mu < M_1$; solid (blue) curve has $M_1 < \mu < M_2$, and the short dashed (green)
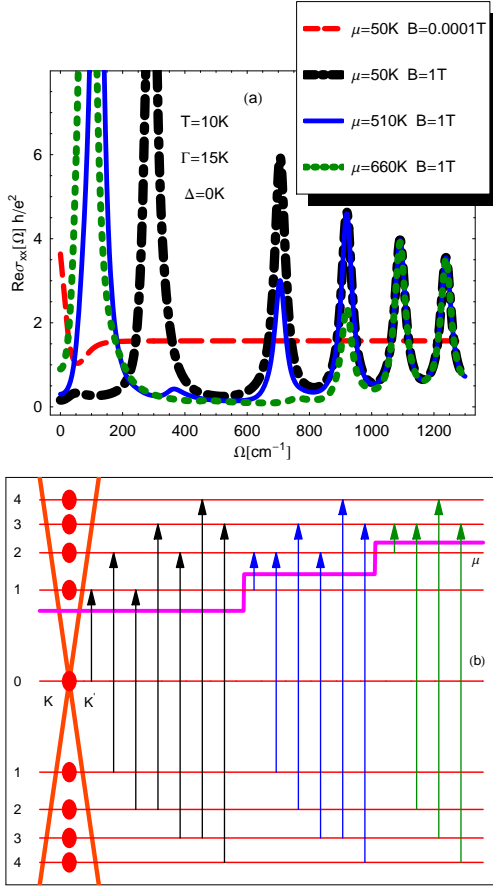
FIG. 1: The absorption peaks and corresponding transitions. (a) Real part of the conductivity, $\mathrm{Re}\,\sigma_{xx}(\Omega)$ in units of e^2/h vs frequency Ω in cm^{-1} for temperature $T = 10\mathrm{K}$ and scattering rate $\Gamma = 15\mathrm{K}$. Long dashed (red), the chemical potential $\mu = 50\mathrm{K}$ and the magnetic field $B = 10^{-4}\mathrm{T}$, dash-dotted (black) $\mu = 50\mathrm{K}$, solid (blue) $\mu = 510\mathrm{K}$, short dashed (green) $\mu = 660\mathrm{K}$ all three for $B = 1\mathrm{T}$. (b) A schematic of the allowed transitions between LLs $n = 0, 1, \ldots 4$ shown as heavy (red) dots for both positive and negative Dirac cones. The pair of cones at points $\mathbf{K}$ and $\mathbf{K}'$ in the Brillouin zone (see Fig. 3 (b)) are combined. Three values of chemical potential are shown as the (violet) heavy solid line. At the left, μ falls between M_0 and M_1; middle, between M_1 and M_2; and on the right, between M_2 and M_3. The first line on the left which corresponds to the first peak in dash-dotted line in upper panel is unusual in that it arises from both interband and intraband transitions and ceases to occur for all other values of chemical potential, while all other interband lines first drop to half their intensity before disappearing entirely as μ crosses to higher energy levels.

curve has $M_2 < \mu < M_3$. The curves remain essentially unchanged for any values of μ between M_N and M_{N+1} and evolve rapidly from one pattern to the next as a new LL is crossed, for a change in chemical potential of order T or Γ whichever is greater.

Referring to Fig. 1(a), in the dash-dotted (black) curve the lowest energy peak is at M_1 and the others at $M_1 + M_2$, $M_2 + M_3$, ... all correspond to interband tran-

sitions from negative to positive Dirac cones. As μ is increased to cross the $n = 1$ LL [solid (blue) curve], the first peak in the dash-dotted (black) curve disappears and the intensity of the next higher peak drops to half its value, while all other peaks remain the same. In addition, a new intraband peak appears at $M_2 - M_1$ and its intensity picks up the lost optical spectral weight from the missing and/or reduced interband transitions. Comparing with the short-dashed (green) curve, the first two interband lines have disappeared, the third has halved and the intraband transition is at $M_3 - M_2$. The first line of the interband series is different in that it never appears with half intensity, while the others do. It is the only one which can be considered as involving both interband and intraband transitions as can be seen in Fig. 1 (b). The energy level schematic shown in this figure summarizes our results. It shows how the first interband line on the far left appears alone, while all others come in pairs. This transition exists only for values of the chemical potential less than M_1, while the others first drop to half intensity as another LL is crossed before disappearing at the next crossing. To verify these predictions optical
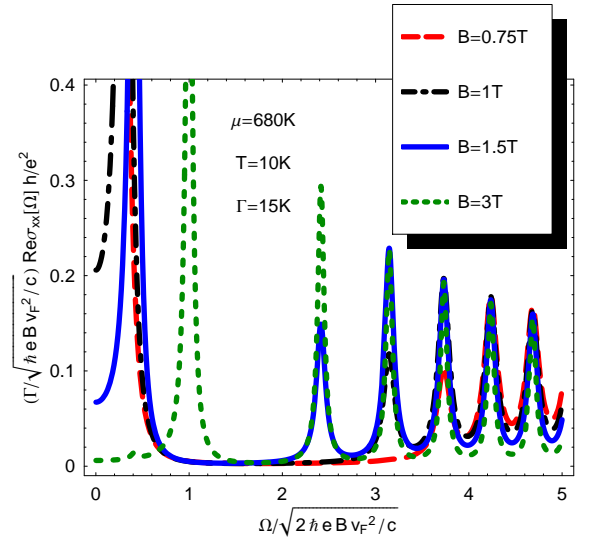

FIG. 2: Real part of the longitudinal conductivity, $\mathrm{Re}\,\sigma_{xx}(\Omega)$ in units of e^2/h multiplied by $\Gamma/\sqrt{\hbar e B v_F^2/c}$ as a function of normalized photon energy $\Omega/\sqrt{2\hbar e B v_F^2/c}$. The temperature is $T = 10\mathrm{K}$, the scattering rate $\Gamma = 15\mathrm{K}$ and the chemical potential $\mu = 680\mathrm{K}$. The long dashed (red) curve is for $B = 0.75\mathrm{T}$, dash-dotted (black) for $B = 1\mathrm{T}$, solid (blue) for $B = 1.5\mathrm{T}$ and short-dashed (green) for $B = 3\mathrm{T}$.

experiments on graphene based field effect device would allow one to change the chemical potential as in Fig. 1 through a change in gate voltage. Such optical experiments have been reported by Li el $al.$[15] in organic metals. It is however also possible to get the same information for a fixed chemical potential if $\mathrm{Re}\,\sigma_{xx}(\Omega)$ is measured at a few well chosen values of the external magnetic field B. This is illustrated in Fig. 2. To see the desired effect

it was convenient to normalize Ω to $\sqrt{2\hbar eBv_F^2/c}$ and to multiply the vertical scale by the dimensionless quantity $\Gamma/\sqrt{\hbar eBv_F^2/c}$. This arrangement guarantees that the various interband lines will all fall at the same normalized value of $\Omega/\sqrt{2\hbar eBv_F^2/c}$ and the intensity of the various lines follow the same pattern as in Fig. 1.

To understand the intensity that is to be assigned to the various lines and their changes with μ it is sufficient to take the limit $T \to 0$ in Eq. (1). For chemical potential $\mu \in [M_N, M_{N+1}]$ we find $(\Omega > 0)$

$$
\operatorname{Re}\sigma_{xx}(\Omega) = \frac{e^2}{h} M_1 \frac{\pi}{2}
$$

$$
\sum_{n=0}^{\infty} \left\{ \begin{bmatrix} 0 & \text{for} & n < N \\ 1 & \text{for} & n = N \\ 2 & \text{for} & n > N \end{bmatrix} \frac{\delta(M_n + M_{n+1} - \Omega)}{\sqrt{n+1} + \sqrt{n}} \right.
$$

$$
\left. + \begin{bmatrix} 1 & \text{for} & n = N \\ 0 & \text{for} & n \neq N \end{bmatrix} \frac{\delta(M_n - M_{n+1} + \Omega)}{\sqrt{n+1} - \sqrt{n}} \right\},
$$

$$(2)$$

where the first and second terms give the interband and intraband transitions, respectively, at the energies indicated by the δ-functions. The denominators come from the $1/\Omega$ factor in Eq. (1). In units of $(e^2/h)M_1(\pi/2)$ which goes like $\sqrt{B}$, the optical spectral weight of various lines is given by the quantities multiplying δ-functions in Eq. (2). For $N > 0$ all interband lines below $n = N$ are missing and the intensity of the line at $n = N$ is half of $2/(\sqrt{n+1} + \sqrt{n})$. The total optical spectral weight lost is

$$
\sum_{n=0}^{N-1} \frac{2}{\sqrt{n+1} + \sqrt{n}} + \frac{1}{\sqrt{N+1} + \sqrt{N}} = \frac{1}{\sqrt{N+1} - \sqrt{N}}.
$$

$$(3)$$

The right hand side is exactly the intensity of the corresponding intraband line given by the second term in (2). We verified that the integrated optical spectral weight under $\operatorname{Re}\sigma_{xx}(\Omega)$ up to energy Ω_{max} is linear in Ω_{max} and approximately equal to $(e^2/h)(\pi/2)\Omega_{max}$ provided Ω_{max} is taken large enough for many LLs to be involved. This linear in Ω_{max} behavior which holds as well for $B = 0$ is another signature of the existence of the Dirac cones. In ordinary metals for $B = 0$ the optical sum would rapidly saturate to a constant value as Ω_{max} is increased beyond the scattering rate Γ. The above rules for the intensity as well as the peculiar behavior of the first inter- (intra-) band line as μ is increased from zero are specific to graphene and as yet have not been verified experimentally, although some data exist as we now describe. The early magneto-reflectance data[16] in fields of order of 1 to 10 T in graphite assigned LL lines to the H-point in the Brillouin zone. Some of these have central frequencies which vary as the square root[17] of B as expected in graphene. More recent data by Li et al.[19] who use high fields up to 20 T, show conventional linear in B behavior. However, very recently, infrared transmission data[18] on ultrathin epitaxial graphite samples[20] in fields up to 4 T have become available and provide $\operatorname{Re}\sigma_{xx}(\Omega)$. A $\sqrt{B}$
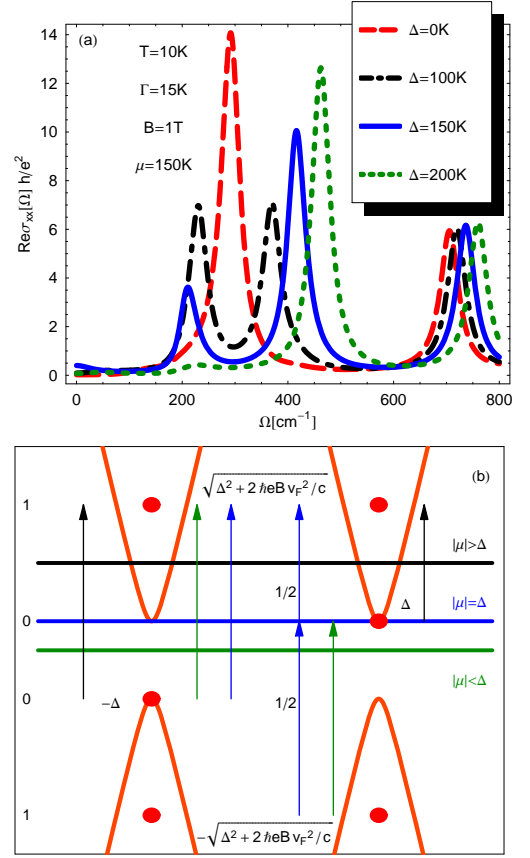

FIG. 3: The absorption peaks and the corresponding transitions when the lowest LL is split. (a) Real part of the longitudinal conductivity, $\operatorname{Re}\sigma_{xx}(\Omega)$ in units of e^2/h vs frequency Ω in cm^{-1} for temperature $T = 10$K, $\Gamma = 15$K, $B = 1$T and chemical potential $\mu = 150$K for 4 values of the excitonic gap Δ. Long dashed (red) $\Delta = 0$K, dash-dotted (black) $\Delta = 100$K, solid (blue) $\Delta = 150$K, short dashed (green) $\Delta = 200$K. (b) Possible optical transitions between LLs with an excitonic gap Δ. Two pairs of cones at $\mathbf{K}$ and $\mathbf{K}'$ points in the Brillouin zone are drawn. Only LLs with $n = 0$ with energies $-\Delta$ (at $\mathbf{K}$ point) and Δ (at $\mathbf{K}'$ point), and $n = 1$ with energies $\pm M_1$, respectively, are shown. Three values of chemical potential are considered $|\mu| < \Delta$ (green), $\mu = \Delta$ (blue) and $|\mu| > \Delta$ (black). For the case $\mu = \Delta$ the state at energy $E_0 = \Delta$ is both occupied and unoccupied with probability $1/2$.

scaling for both the energy and the intensity of the first line was taken as evidence for Dirac quasiparticles. In view of the known sensitivity of some properties to coupling between layers it is not obvious that the various carbon sheets in the samples are sufficiently decoupled to be treated as isolated graphene sheets[17]. Further, to understand the results it is necessary to assume that there is a variation in charging, i.e. each sheet can have different chemical potential. We have analyzed the intensities of the one intraband and of the three interband transitions reported in[18]. The intensity of the first interband line (B) in Fig. 1 of Ref.[18], which can occur only for $|\mu| < M_1$, is

the largest and that of the intraband line (A) is smaller by a factor of 0.36. This can only be understood if there are at least three times more sheets for which the chemical potential falls below M_1 than above. Further, the ratio of the intensity of the second (C) and the third (D) interband lines to the first (B) are 0.34 and 0.19, respectively. These values are somewhat smaller than 0.41 and 0.32 expected from our theory, coming from the sheets with $|\mu| < M_1$. Adding in the other sheets with $|\mu| > M_1$ only increase the above discrepancy, because they add to the second and third interband lines, but not to the first. While the above provides some indirect support of our theory, further experiments are needed to verify the main features described here. A case for further studies is a bilayer[21] where it is known[8] that the two lowest LLs both lie at zero energy and this should change the pattern of behavior of the absorption lines described here.

The ac conductivity may also be used to get information on the opening of a possible gap related to the sublattice symmetry breaking in graphene[4,13,14,22,23,24]. In Fig. 3 (a) we show results for $\mathrm{Re}\,\sigma_{xx}(\Omega)$ plotted using the generalization of Eq. (1) to finite Γ. Four values of the excitonic gap Δ are considered. For $\Delta < |\mu|$ the single peak at $294\,\mathrm{cm}^{-1}$ has split into two of nearly equal intensity, for $|\mu| = \Delta$ the lower peak has approximately $1/3$ the intensity of the upper peak and for $\Delta > |\mu|$ a single peak is seen at the higher energy. Fig. 3 (b) gives a schematic of the levels involved and shows the transitions. For convenience we have fixed the gap in the figure and considered three values of chemical potential. For $|\mu| < \Delta$ the interband transition $-M_0$ to M_1 (LHS cone) and $-M_1$ to M_0 (RHS cone) are both possible and have the same energy $M_1 + \Delta$, so only one line is seen shifted to higher energy. For $|\mu| = \Delta$ one needs to account for the fact that the state at $n = 0$ (RHS cone) is occupied (unoccupied) with probability $1/2$. The possible interband transitions are $-M_0$ to M_1 (LHS cone) with energy $M_1 + \Delta$ and $-M_1$ to

M_0 with energy $M_1 + \Delta$, and an intraband transition of M_0 to M_1 with energy $M_1 - \Delta$ (RHS cone) each weighted by $1/2$ rather than by 1. This gives a 3 to 1 ratio favoring the higher energy line. Finally, for $|\mu| > \Delta$, the $-M_0$ to M_1 interband transition (LHS) has energy $M_1 + \Delta$ and the intraband transition of M_0 to M_1 (RHS) has energy $M_1 - \Delta$. The two lines have nearly the same intensity. It is clear that optics provides a useful probe for observing various kinds of gaps and here the excitonic gap is taken as an example.

In summary, we have found an anomaly in the first absorption peak in the optical conductivity of graphene. When the chemical potential, tunable by the gate voltage, sweeps through the various LL energies, this peak never halves its intensity before disappearing while the other lines do. This pattern of behavior is specific to the Dirac nature of quasiparticles in graphene and should be easily observable in the experiments. It originates from the special structure of LLs in graphene, where each positive energy level has its negative counterpart, except for the zero energy lowest LL. For the Shubnikov de Haas oscillations[25] this structure of LLs resulted in a phase shift of π used to identify these quasiparticles in the dc measurements[2,3]. Furthermore, should an excitonic gap open in high magnetic field, its presence will lead to a specific signature in an ac optical experiment. For $\Delta < |\mu| < M_1$, the $n = 0$ to $n = 1$ transition will split into two lines of nearly equal intensity, while for $|\mu| = \Delta$ the intensity ratio of higher to lower energy line will be about 3. For $|\mu| < \Delta$ the line will simply shift upward without splitting.

[1] K.S. Novoselov *et al.*, Science **306**, 666 (2004)

[2] K.S. Novoselov *et al.*, Nature **438**, 197 (2005).

[3] Y. Zhang *et al.*, Nature **438**, 201 (2005).

[4] Y. Zhang *et al.*, Phys. Rev. Lett. **96**, 136806 (2006).

[5] Y. Zheng and T. Ando, Phys. Rev. B **65**, 245420 (2002).

[6] V.P. Gusynin and S.G. Sharapov, Phys. Rev. Lett. **95**, 146801 (2005).

[7] N.M.R. Peres, F. Guinea, and A.H. Castro Neto, Phys. Rev. B **73**, 125411 (2006).

[8] K.S. Novoselov *et al.*, Nature Physics **2**, 177 (2006).

[9] G.W. Semenoff, Phys. Rev. Lett. **53**, 2449 (1984).

[10] F.D.M. Haldane, Phys. Rev. Lett. **61**, 2015 (1988).

[11] V.P. Gusynin and S.G. Sharapov, Phys. Rev. B **73**, 245411 (2006).

[12] V.P. Gusynin, S.G. Sharapov and J.P. Carbotte, Phys. Rev. Lett. **96**, 256802 (2006).

[13] D.V. Khveshchenko, Phys. Rev. Lett. **87**, 206401 (2001); *ibid.* **87**, 246802 (2001).

[14] E.V. Gorbar, V.P. Gusynin, V.A. Miransky, and I.A. Shovkovy, Phys. Rev. B **66**, 045108 (2002).

[15] Z.Q. Li *et al.*, Nano Letters **6**, 224 (2006).

[16] W.W. Toy, M.S. Dresselhaus, and G. Dresselhaus, Phys. Rev. B **15**, 4077 (1977).

[17] D.N. Basov has pointed out to us that the two main transitions in[18] agree well with the data of Toy *et al.*[16] on graphite.

[18] M.L. Sadowski *et al.*, Phys. Rev. Lett. **97**, 266405 (2006).

[19] Z.Q. Li *et al.*, Phys. Rev. B **74**, 195404 (2006).

[20] C. Berger *et al.*, Science **312**, 1191 (2006).

[21] D.S.L. Abergel, V.I. Fal'ko, Preprint cond-mat/0610673.

[22] K. Nomura and A. H. MacDonald, Phys. Rev. Lett. **96**, 256602 (2006).

[23] J. Alicea and M.P.A. Fisher, Phys. Rev. B **74**, 075422 (2006).

[24] V.P. Gusynin, V.A. Miransky, S.G. Sharapov, and I.A. Shovkovy, Phys. Rev. B 74, 195429 (2006).

[25] V.P. Gusynin and S.G. Sharapov, Phys. Rev. B **71**, 125124 (2005).